Response of liquid ^{3}He at finite temperatures

M. Barranco
Departament d'Estructura i Constituents de la Matèria, Facultat de Física, Universitat de Barcelona, E-08028 Barcelona, Spain

E. S. Hernández
Departamento de Física, Facultad de Ciencias Exactas y Naturales, Universidad de Buenos Aires, and Consejo Nacional de Investigaciones Científicas y Técnicas, RA-1428 Buenos Aires, Argentina

J. Navarro
Instituto de Física Corpuscular (CSIC-Universitat de València), Facultat de Física, E-46100 Burjassot, València, Spain
(Received 2 January 1996)

The random-phase-approximation (RPA) dynamical response of liquid ^{3}He at finite temperatures has been calculated using an effective density-dependent atom-atom interaction. The interaction contains a zero-range part of Skyrme type, supplemented by a weighted density approximation to account for short-range correlations, and a long-range effective interaction of Lennard-Jones type. The calculated zero-sound and paramagnon energy centroids agree reasonably with data, and the calculated strength exhibits a negative energy tail extending up to -0.5 meV, also in good agreement with existing data. We have found that opposite to what happens with zero sound, within RPA the paramagnon peak is rather insensitive to thermal broadening. [S0163-1829(96)01133-2]

I. INTRODUCTION

Since the pioneering work of Stringari,[1] an effective Skyrme-like atom-atom interaction has been used for the study of bulk and surface properties of liquid ^{3}He, as well as for energy systematics and the shell structure of ^{3}He droplets,[2,3] and for the density-density response of drops[4] and homogeneous liquid.[5] The use of a phenomenological approach seems appropriate to explore physical situations where a microscopic calculation is difficult to carry out. This explains why the Landau theory of Fermi liquids is so widely used to study the response to an external probe in the long-wavelength–low-frequency limit; a successful alternative, which removes the restriction to low transferred momentum intrinsic to the Landau view, is contained in the polarization potential theory of Pines.[6] However, it is worth noting that while these approaches assume a previous knowledge of the ground state structure of the system, out of which the spectrum of elementary excitations can be constructed, a phenomenological density-dependent interaction allows a simultaneous analysis of both ground state and excitation properties.

The density functional adequate to describe most aspects of the static and dynamic behavior of liquid helium is not unique. The former determinations[1–3] took into account bulk data in the density channel such as the equation of state at zero temperature and the effective mass of helium atoms, disregarding the spin-dependent part of the interaction. It was later seen[7] that in order to reproduce the experimental trend of the Landau parameters in the antisymmetric spin channel, interaction terms depending upon spin density were needed. The anomalous dispersion of the zero-sound mode was correctly described incorporating a finite-range term,[5] following a proposal by Dupont-Roc *et al.*[8] for liquid ^{4}He; a similar viewpoint, inspired in polarization potential theory, was undertaken by Weisgerber and Reinhard.[9] Furthermore, in Ref. 10 an explicit dependence of the functional on the spin current density was proposed; this form was later employed to investigate the structure and pairing properties of helium drops.[11]

Experimental data and several model calculations of the dynamical structure factor $S(q,\omega)$ of liquid ^{3}He have been recently reviewed by Glyde;[13] in addition, random-phase-approximation (RPA) calculations at zero temperature have been presented in Refs. 5 and 9. To the best of our knowledge, finite-temperature RPA calculations in liquid ^{3}He have not yet been performed; as pointed out in Ref. 13, previous RPA-like estimates of the response, based on the free Lindhard function χ_0 with an effective mass 3 times larger than the bare mass of a helium atom, yield a first, however limited, description of the excitations. In the approach undertaken by Glyde and Khanna,[14] the susceptibility has been computed at 15 mK according to its expression in the Landau limit, in terms of the Landau parameters, replacing the corresponding susceptibility $\chi_0^{(L)}$ by the Lindhard function.

Our present goal is to investigate the response of liquid ^{3}He at finite temperatures in the frame of the RPA theory presented in Ref. 5. This formalism, originally developed for the zero-temperature case, has been recently generealized to thermally excited systems in an application to symmetric nuclear matter;[12] we wish to stress here that for Skyrme-like interactions, exchange terms are automatically included. This exact RPA treatment gives the correct Landau limit[5] and beyond the long-wavelength regime, generalized temperature-dependent Lindhard functions appear in the dynamical susceptibility, as well as the full momentum dependence of the multipolar amplitudes of the effective interaction.

In order to compute the response in the liquid, some modifications to the form of the functional of Refs. 10 and

11 are required to restore translational invariance, to the cost of a new adjustment in the parameters. The present parametrization guarantees an excellent fit of all bulk properties, of the dispersion curve of zero sound at zero temperature and various pressures, of the dependence of the symmetric and antisymmetric Landau parameters with the density of the liquid, and of the stability of drops within a wide range of sizes. The location of the low-temperature paramagnon peak as a function of incoming momentum is also reasonably reproduced. This functional is then introduced as an input for dynamical susceptibility calculations in the spirit of Ref. 12, and we examine the predictions for zero sound and paramagnon peaks, for different temperatures and momenta.

This paper is organized as follows. In Sec. II we present the effective Skyrme-like force and the particle-hole (ph) interaction produced by double functional differentiation of the total Hartree-Fock energy. The parametrization differs from the one in Ref. 11 only in the strengths and exponents for the spin channel; the fit to the symmetric Landau parameters is thus the same as in this previous work, and we show the adjustment of the magnetic parameters. In Sec. III we display the results obtained for the response at finite temperatures; as in Ref. 12, the thermal effects appear only in the ph propagators involved in the RPA equations, since the current interaction does not depend upon temperature. Section IV contains the summary.

II. EFFECTIVE PARTICLE-PARTICLE AND PARTICLE-HOLE INTERACTIONS

The atom-atom effective interaction employed in this work is similar to the one presented in Ref. 11, slightly modified to guarantee Galilean invariance, and reads

$$V(1,2)=\mathcal{V}_0\delta(\mathbf{r}_{12})+\frac{1}{2}[\mathbf{k}'^2\mathcal{V}_1\delta(\mathbf{r}_{12})+\delta(\mathbf{r}_{12})\mathcal{V}_1\mathbf{k}^2]+\mathbf{k}'\cdot\mathcal{V}_2\delta(\mathbf{r}_{12})\mathbf{k}, \tag{1}$$

where $\delta(\mathbf{r}_{12})$ is the delta function $\delta(\mathbf{r}_1-\mathbf{r}_2)$, $\mathbf{k}$ is the operator $(\nabla_1-\nabla_2)/2\imath$ acting on the right, and $\mathbf{k}'$ is the operator $-(\nabla_1-\nabla_2)/2\imath$ acting on the left. The functions $\mathcal{V}_i$ depend on the densities in the following manner:

$$\mathcal{V}_0=t_0+t_0'\tilde{\rho}^\gamma+u_0\tilde{\rho}^\beta\mathbf{S}\cdot\mathbf{S}+v_0(\mathbf{J}\cdot\mathbf{J}-\mathbf{S}\cdot\mathbf{T}), \tag{2}$$

$$\mathcal{V}_1=t_1+t_1'\tilde{\rho}+u_1\mathbf{S}\cdot\mathbf{S}+v_1(\mathbf{J}\cdot\mathbf{J}-\mathbf{S}\cdot\mathbf{T}), \tag{3}$$

$$\mathcal{V}_2=t_2+t_2'\tilde{\rho}+u_2\mathbf{S}\cdot\mathbf{S}+v_2(\mathbf{J}\cdot\mathbf{J}-\mathbf{S}\cdot\mathbf{T}). \tag{4}$$

The various densities appearing in this expression are related to the single-particle density matrix $\rho(\mathbf{r},\sigma;\mathbf{r}',\sigma')$, where σ and $\sigma'=\pm 1/2$, as follows.

Particle density:

$$\rho(\mathbf{r})=\sum_\sigma \rho(\mathbf{r},\sigma;\mathbf{r}',\sigma)|_{\mathbf{r}=\mathbf{r}'}. \tag{5}$$

Spin density:

$$\mathbf{S}(\mathbf{r})=\sum_{\sigma,\sigma'}\rho(\mathbf{r},\sigma;\mathbf{r}',\sigma')\langle\sigma'|\vec{\sigma}|\sigma\rangle|_{\mathbf{r}=\mathbf{r}'}. \tag{6}$$

Spin-kinetic-energy density:

$$\mathbf{T}(\mathbf{r})=\sum_{\sigma,\sigma'}|\nabla\rho(\mathbf{r},\sigma;\mathbf{r}',\sigma')|^2\langle\sigma'|\vec{\sigma}|\sigma\rangle|_{\mathbf{r}=\mathbf{r}'}. \tag{7}$$

Spin-current-tensor density:

$$\mathbf{J}(\mathbf{r})=\frac{1}{2\imath}\sum_{\sigma,\sigma'}(\nabla-\nabla')\rho(\mathbf{r},\sigma;\mathbf{r}',\sigma')\langle\sigma'|\vec{\sigma}|\sigma\rangle|_{\mathbf{r}=\mathbf{r}'}, \tag{8}$$

where $\vec{\sigma}$ is the Pauli matrices vector. Furthermore, in Eqs. (2)–(4), $\tilde{\rho}$ is a coarse-grained density defined as

$$\tilde{\rho}(\mathbf{r})=\int d\mathbf{r}'w(\mathbf{r}-\mathbf{r}')\rho(\mathbf{r}'), \tag{9}$$

where the weight function is taken as

$$w(\mathbf{r})=\begin{cases}\dfrac{3}{4\pi h^3}, & r<h,\\ 0, & r>h,\end{cases} \tag{10}$$

and the range h is a free parameter.

In the case of a homogeneous nonpolarized system, the densities (6)–(8) vanish and $\tilde{\rho}=\rho$. But all these densities are important to determine the ph interaction, which can be obtained through a second functional derivative of the total energy with respect to the occupation numbers. We can write the ph matrix elements in the following manner:

$$\langle\mathbf{q}+\mathbf{q}_1,\mathbf{q}_2|V_{\rm ph}|\mathbf{q}_1,\mathbf{q}+\mathbf{q}_2\rangle=V_{\rm ph}^{(0)}P_{(0)}+V_{\rm ph}^{(1)}P_{(1)}, \tag{11}$$

where $P_{(S)}$ are the spin-symmetric ($S=0$) and spin-antisymmetric ($S=1$) projector operators. For the effective particle-particle interaction (1), the general form of $V_{\rm ph}^{(S)}$ is[5]

$$V_{\rm ph}^{(S)}=W_1^{(S)}(q)+W_2^{(S)}(q)(\mathbf{q}_1-\mathbf{q}_2)^2+W_3^{(S)}(q)[\mathbf{q}_1\cdot(\mathbf{q}+\mathbf{q}_2)+\mathbf{q}_2\cdot(\mathbf{q}+\mathbf{q}_1)]. \tag{12}$$

Denoting by $\omega(q)$ the Fourier transform of the weight function $w(r)$, we obtain the following form for the functions $W_i^{(S)}$ For the coherent $S=0$ channel,

$$W_1^{(0)}=t_0+t_0'\rho^\gamma[1+2\gamma\omega(q)+\tfrac{1}{2}\gamma(\gamma-1)\omega^2(q)]+\tfrac{3}{10}(t_1'+3t_2')\omega(q)\rho k_F^2+\tfrac{1}{4}\{(t_1-3t_2)+[1+\omega(q)](t_1'-3t_2')\rho\}q^2, \tag{13}$$

$$W_2^{(0)}=\tfrac{1}{4}\{(t_1+3t_2)+[1+\omega(q)](t_1'+3t_2')\rho\}, \tag{14}$$

$$W_3^{(0)}=\tfrac{1}{4}\omega(q)(t_1'+3t_2')\rho, \tag{15}$$

where $k_F=(3\pi^2\rho)^{1/3}$ indicates the Fermi momentum, while those in the incoherent $S=1$ channel now read

$$W_1^{(1)}=-(t_0+t_0'\rho^\gamma)-\tfrac{1}{4}[(t_1+t_2)+(t_1'+t_2')\rho]q^2+\rho^2[u_0\rho^\beta+\tfrac{3}{10}(u_1+3u_2)k_F^2]+\tfrac{1}{4}\rho^2[v_0+\tfrac{3}{10}(v_1+3v_2)k_F^2]q^2, \tag{16}$$

$$W_2^{(1)} = -\tfrac{1}{4}[(t_1-t_2)+(t_1'-t_2')\rho] - \tfrac{1}{2}\rho^2[v_0+\tfrac{3}{10}(v_1+3v_2)k_F^2], \quad (17)$$

$$W_3^{(1)} = 0. \quad (18)$$

Finite-range effects can be introduced in this description, replacing the interaction term $t_0\delta(\mathbf{r})$ by the direct matrix element of a screened Lennard-Jones (SLJ) potential[5,8] in the spin-symmetric channel:

$$V(r) = \begin{cases} 4\epsilon\left[\left(\dfrac{\sigma}{r}\right)^{12} - \left(\dfrac{\sigma}{r}\right)^{6}\right], & r \geqslant \sigma, \\ \dfrac{3+n}{n}\left[\dfrac{8\epsilon}{3} + \dfrac{3t_0}{8\pi\sigma^3}\right]\left[1-\left(\dfrac{r}{\sigma}\right)^{n}\right], & r \leqslant \sigma. \end{cases} \quad (19)$$

The height of the core is fixed so that the volume integral of $V(r)$ is $t_0/2$, thus guaranteeing that the bulk properties of both finite- and zero-range functionals are the same. This prescription for the inclusion of finite-range effects leads to replacement of $t_0/2$ by $V_{\mathrm{SLJ}}(q)$, the Fourier transform of the SLJ potential, in $W_1^{(0)}$ given by Eq. (13). The finite-range density functional thus obtained has been successful in accounting for anomalous zero-sound dispersion at saturation pressure[5] as well as for finite pressures.[11]

The Landau fields can be straighforwardly obtained from Eq. (12), taking $q_i = k_F$ and $\mathbf{q}\cdot\mathbf{q}_i = 0$, and they read

$$f_0^s(q) = V_{\mathrm{SLJ}}(q) + \tfrac{1}{2}t_0'\rho^\gamma[1+2\gamma\omega(q)+\tfrac{1}{2}\gamma(\gamma-1)\omega^2(q)] + \tfrac{1}{4}\left[t_1+3t_2+\frac{5+8\omega(q)}{5}(t_1'+3t_2')\rho\right]k_F^2 + \tfrac{1}{8}[(t_1-3t_2)+([1+\omega(q)]t_1'-3t_2'),\rho]q^2, \quad (20)$$

$$f_1^s(q) = -\tfrac{1}{4}[t_1+3t_2+(t_1'+3t_2')\rho]k_F^2. \quad (21)$$

As shown in previous works[10,11] the spin and spin-current density contribution are needed to reproduce the density dependence of the spin-antisymmetric Landau fields f_0^a and f_1^a, whose expression for the above effective interaction is

$$f_0^a(q) = -\tfrac{1}{2}(t_0+t_0'\rho^\gamma) - \tfrac{1}{4}[(t_1-t_2)+(t_1'-t_2')\rho]k_F^2 - \tfrac{1}{8}[(t_1+t_2)+(t_1'+t_2')\rho]q^2 + \tfrac{1}{2}\rho^2[u_0\rho^\beta+\tfrac{3}{10}(u_1+3u_2)k_F^2] - \tfrac{1}{2}\rho^2[v_0+\tfrac{3}{10}(v_1+3v_2)k_F^2][k_F^2-\tfrac{1}{4}q^2], \quad (22)$$

$$f_1^a(q) = \tfrac{1}{4}[(t_1-t_2)+(t_1'-t_2')\rho]k_F^2 + \tfrac{1}{2}\rho^2[v_0+\tfrac{3}{10}(v_1+3v_2)k_F^2]k_F^2. \quad (23)$$

TABLE I. Parameters of the effective interaction. $\rho_0 = 0.016\,348\,9$ Å^{-3} is the experimental saturation density.

t_0	$t_0'\rho_0^\gamma$	t_1	t_2
(K Å^3)	(K Å^3)	(K Å^5)	(K Å^5)
-1369.351	496.3449	-772.236	-772.236
$t_1'\rho_0$	$t_2'\rho_0$	$u_0\rho_0^2$	$(u_1+3u_2)\rho_0^2$
(K Å^5)	(K Å^5)	(K Å$^{3(1+\beta)}$)	(K Å$^{5(1+\beta)}$)
96.0680	160.0044	-0.2690275	2011.3517
$v_0\rho_0^2$	$(v_1+3v_2)\rho_0^2$	ϵ	σ
(K Å$^{3(1+\beta)}$)	(K Å$^{5(1+\beta)}$)	(K)	(Å)
-399.5911	1628.351	6	2.91
h (Å)	γ	β	n
4.3	2.1251	-2.085	8

The corresponding Landau parameters are given by the values of these fields at $q=0$.

It is then clear that in our approach finite-range effects manifest themselves only in the $S=0$ channel, through the coarse-grained density, represented by the weighting function $w(q)$, and also through the screened Lennard-Jones potential $\mathrm{V_{SLJ}}$. The parameters of the effective interaction (1) are displayed in Table I. They have been revised, with respect to those presented in Ref. 11, in order to yield the best possible fit of the dispersion relation of zero sound at vanishing temperature and pressures $P=0$, 5, 10, and 20 bars, according to the formalism presented in the next section, as well as of the magnetic Landau parameters for densities ranging between saturation and fusion at zero temperature. The latter are shown in Fig. 1, and it can be seen that there is an excellent agreement with the data from Ref. 15; notice, however, that F_1^a is not experimentally known, and that only sum rule estimates are available.

III. RPA RESPONSE FUNCTION

The calculation of the response in the RPA at zero temperature starting from effective interactions of the type (1) has been presented in Ref. 5 and more recently[12] the formalism has been generalized to finite temperature T and applied to thermally excited symmetric nuclear matter. The dynamical susceptibility for each spin channel S is the solution of the RPA integral equation and, for effective interactions of the form (1), it can be written in the form

$$\chi^{(S)}(q,\omega,T) = 2\frac{\chi_0(q,\omega,T)}{D^{(S)}(q,\omega,T)}, \quad (24)$$

where the factor of 2 stands for the spin degeneracy, χ_0 is the Lindhard function, and the denominator is

$$D^{(S)}(q,\omega,T) = 1 - W_1^{(S)}(q)\chi_0 - 2W_2^{(S)}\left[\frac{q^2}{4} - \frac{\omega m^{*2}}{q}\frac{1}{1-(m^*k_F^3/3\pi^2)W_2^{(S)}}\right]\chi_0 + 2W_2^{(S)}\left(\frac{q^2}{2}\chi_0 - k_F^2\chi_2\right) + [W_2^{(S)}k_F^2]^2\left[\chi_2^2 - \chi_0\chi_4 + \left(\frac{\omega m^*}{k_F^2}\right)^2\chi_0^2 - \frac{m^*}{6\pi^2 k_F}q^2\chi_0\right], \quad (25)$$

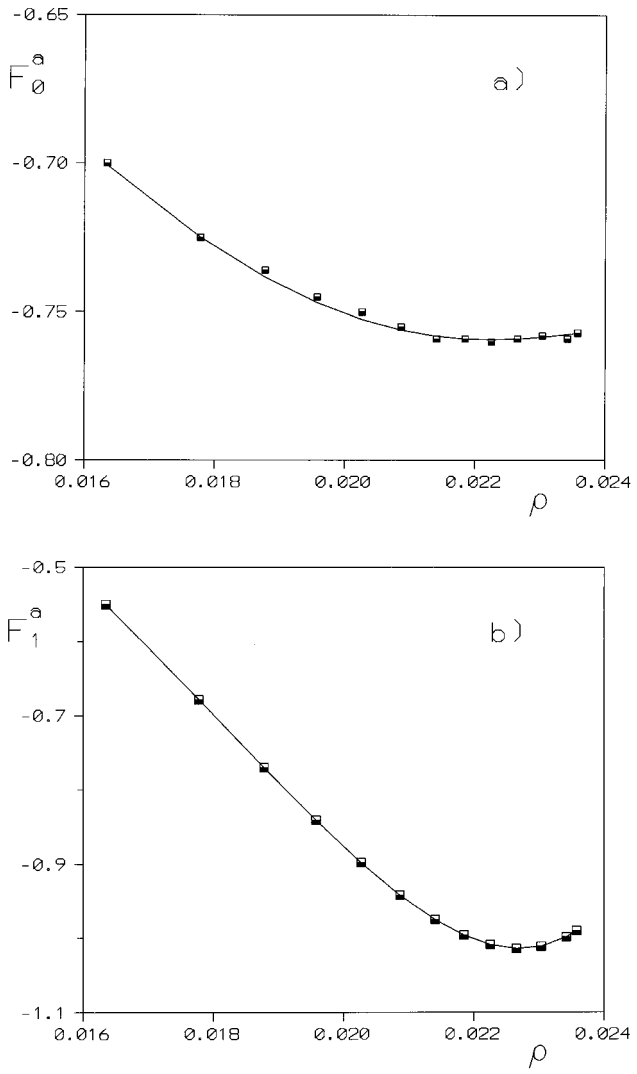

FIG. 1. (a) The magnetic Landau parameter F_0^a as a function of density (in Å^{-3}); (b) same for F_1^a. Experimental data are taken from Ref. 15.

where m^* is the effective mass at density ρ, and the generalized susceptibilities $\chi_2(q,\omega,T)$ and $\chi_4(q,\omega,T)$ have been given in Ref. 12. As shown in Ref. 5, if q and ω approach zero keeping q/ω at a finite figure, the well-known expression for the dynamical response in the Landau limit[16] is obtained.

It should be noticed that in previous works[10,11] the anomalous dispersion of zero sound was estimated by means of sum rules; instead, as in Ref. 5, the present calculation searches the collective pole of the response function (24). At vanishing temperature, the zero-sound energies have been also obtained from the RPA integral equation,[9] starting from a density functional that combines the density and momentum dependence of Skyrme interactions with the finite-range effects contained in the polarization potentials designed by Pines.[6]

In Fig. 2 we show, as solid lines, the computed dispersion relation at $T=0$ together with the experimental data[17] for the values $P=0$, 5, 10, and 20 bars from the lowest- to the highest-lying curve. One can see that the agreement with experiment is good. The short-dashed line represents the upper bound of the ph excitation band for a free Fermi gas with the Fermi momentum $k_F \approx 0.785$ Å^{-1} and effective mass $m^* \approx 2.8m$, which corresponds to the saturation density of liquid ^{3}He. The long and medium dashed lines, respectively, indicate the position of the maximum of the collective strength in the coherent channel $S=0$ at temperatures $T=1.2$ K and $T=\varepsilon_F^*$ with $\varepsilon_F^*=\hbar^2k_F^2/2m^*$ taking the value 1.8 K. At each nonvanishing temperature, the Fermi momentum and the effective mass have been calculated for the density associated with the saturated vapor pressure (SVP). The strength in each spin channel corresponds to the dynamical structure factor $S(q,\omega,T)$ related to the imaginary part of the dynamical susceptibility by the detailed balance relationship[12]

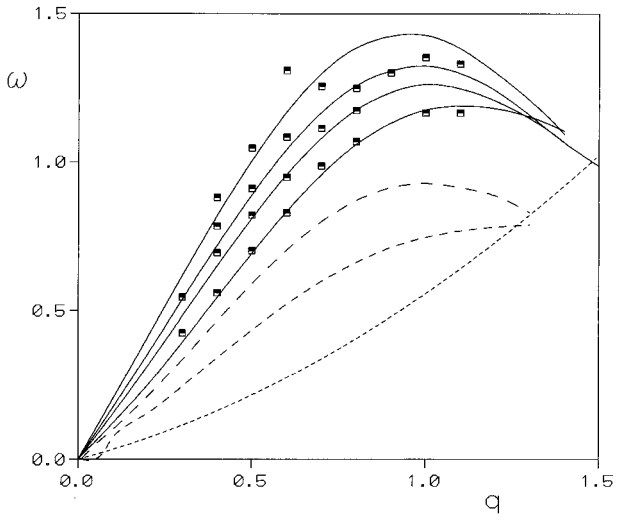

FIG. 2. The dispersion relation of the zero-sound mode of liquid ^{3}He. Solid lines correspond to zero temperature and pressures $P=0$, 5, 10, and 20 bars (from the lowest to the highest curve) together with experimental data (Ref. 17). Long and medium dashed lines, respectively, correspond to temperatures $T=1.2$ K and $T=\varepsilon_F^*$, and the short dashed curve is the upper bound of the ph excitation band. Energies are given in meV and momenta in Å^{-1}.

$$S(q,\omega,T)=-\frac{1}{\pi}\frac{\mathrm{Im}\chi(q,\omega,T)}{1-e^{-\omega/T}}. \tag{26}$$

We can appreciate in Fig. 2 the persistence of a well-defined zero-sound peak for all chosen temperatures up to large transferred momentum q. A close examination of the strength in the symmetric spin channel as a function of both momentum q and energy ω indicates that the dispersion curve crosses the ph band at $q \approx 1.3$ Å^{-1} at all temperatures; at these values, the collective peak and the low-energy resonance merge together in the continuum, in agreement with observed data.[18] This behavior is to be contrasted with that of the antisymmetric spin channel. In Fig. 3 the energy of the peak of the magnetic strength has been depicted as a function of q at SVP for the three temperatures used above. One can see that the paramagnon peak energy is not sensitive to increasing temperature; indeed, as the liquid heats up, the major displacement takes place in the vicinity of $q=k_F$. At zero temperature, the peak energy exhibits a flat structure around $q=0.7$ Å^{-1} which is gradually washed out as T in-

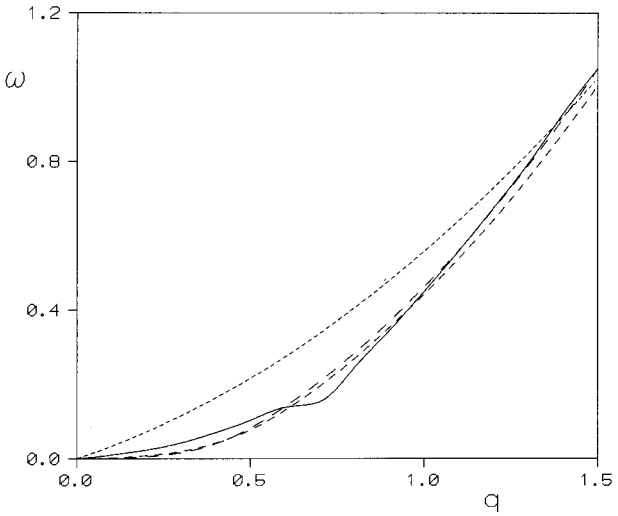

FIG. 3. The dispersion relation for the energy at the peak of the paramagnon strength. Solid, long dashed, and medium dashed curves, respectively, correspond to temperatures $T=0$, 1.2 K, and ε_F^*.

creases. The interaction in the magnetic channel being a weakly attractive one, this structure is just a slight distortion of the curve $\omega_0(q)$ for the maximum of the ph strength of an ideal gas at zero temperature.[20] In fact, in a noninteracting system, for transferred momenta below $2k_F$, the peak of the ph resonance lies at

$$\omega_0(q)=\begin{cases}\dfrac{qk_F}{m^*}-\dfrac{q^2}{2m^*}, & q<k_F,\\ \dfrac{q^2}{2m^*}, & k_F<q<2k_F.\end{cases} \tag{27}$$

We then see that curve $\omega_0(q)$ approaches the matching point at k_F with zero slope from the left, this being the reason of the observed flattening of the $\omega(q)$ curve in the presence of a weak interaction.

While most of the paramagnon dispersion curve lies inside the ph continuum, for the largest values of transferred momentum, a collective peak appears for both $T=0$ and $T=1.2$ K. However, in either case the peak strength is weak, as we can appreciate from Fig. 4, where the maximum strength per particle in the asymmetric spin channel is plotted for the same temperatures as above. The experimental data are taken from Ref. 18.

This maximum strength presents, at zero temperature, a drastic decrease with increasing momentum, as already observed in previous works;[5,11] thermal excitation of the liquid causes the strength to approach zero asymptotically at an even faster rate, and the ordinate at zero momentum is considerably enlarged. This behavior of the ordinates is related to the variation in the densities at SVP for increasing temperature, which can be seen to reach a maximum at $T\approx 0.54$ K. Taking into account the fact that for zero transferred momentum the peak of the paramagnon strength lies at zero energy, its height can be evaluated in the long-wavelength regime[5] as a function of the Landau parameters; indeed, in this limit the denominator of Eq. (24) in the magnetic channel takes the form

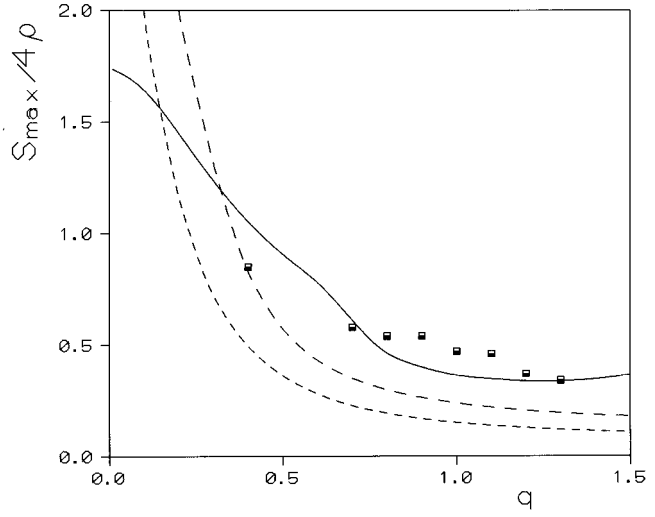

FIG. 4. The peak of the paramagnon strength (in meV^{-1}) as a function of transferred momentum (in Å^{-1}). Solid, long dashed, and medium dashed curves, respectively, correspond to temperatures $T=0$, 1.2 K, and ε_F^*. The experimental data have been taken from Ref. 18.

$$D^{(1)}=1-\frac{2\pi^2}{m^*k_F}\left[F_0^a+\frac{F_1^a}{1+F_1^a/3}\left(\frac{m^*\omega}{qk_F}\right)^2\right]\chi_0. \tag{28}$$

Explicit calculations show that the paramagnon strength is a monotonically increasing function of the density, and consequently, possesses a maximum as a function of temperature at $T\approx 0.54$ K. This is illustrated in Fig. 5. It should be also remarked that insofar as the temperature dependence of the paramagnon peak is concerned, the present results are in good agreement with the dynamical structure factor experimentally observed.[18]

The total strength is defined as

$$S(q,\omega)=S^{(0)}(q,\omega)+\frac{\sigma_c}{\sigma_i}S^{(1)}(q,\omega), \tag{29}$$

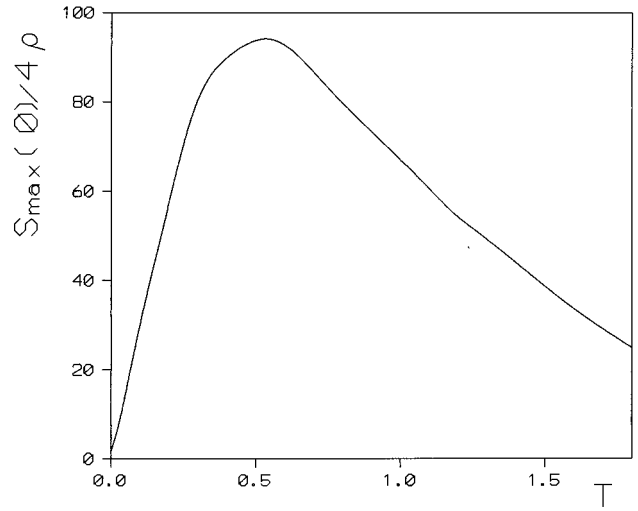

FIG. 5. The peak of the paramagnon strength at zero transferred momentum as a function of temperature. Units are the same as in Fig. 4.

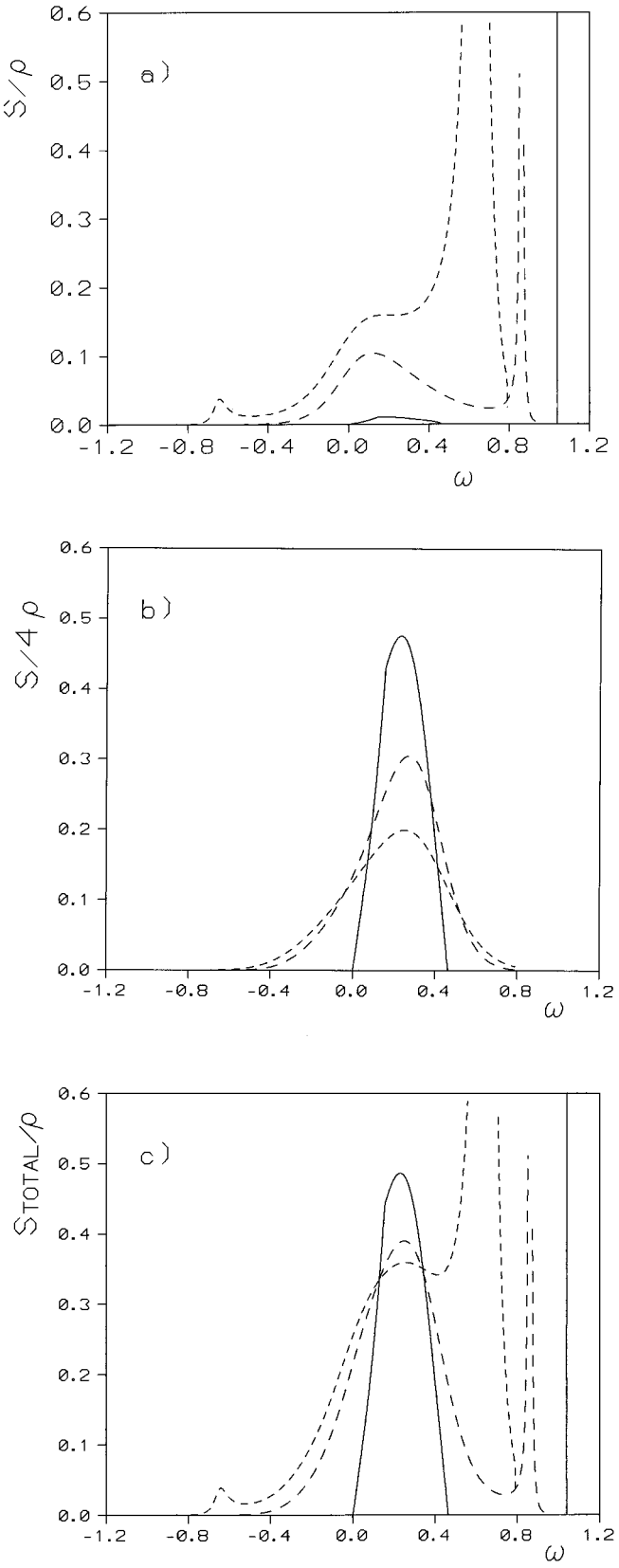

FIG. 6. The strength per particle in meV^{-1} as a function of energy (in meV) (a) in the coherent $S=0$ channel; (b) in the incoherent $S=1$ channel, times the weigthing factor $\sigma_c/\sigma_i=0.25$; (c) the total one. Solid, long dashed, and medium dashed curves, respectively, correspond to temperatures $T=0$, 1.2 K, and ε_F^*.

where $\sigma_{c,i}$ are the coherent and incoherent cross sections for neutron scattering with ratio $\sigma_c/\sigma_i=0.25$. Figure 6, respectively contains (a) the strength $S^{(0)}$, (b) one-fourth of the incoherent $S^{(1)}$ strength, and (c) the total one given in Eq. (29), per particle and as functions of transferred energy for a momentum $q=k_F$ and for temperatures $T=0$, 1.2 K, and ε_F^* It is clearly seen that the paramagnon peak dominates the continuum strength and that the location of the resonance maximum is rather insensitive to thermal excitation, as already indicated in Fig. 3. By contrast, the collective peak in the density channel undergoes an important thermal broadening as well as a displacement towards lower energies in agreement with the results in Fig. 2. An interesting feature of these figures, which extend over the whole energy axis rather than over the positive energy region, is the fact that for sufficiently high temperatures an ''image peak'' of the collective mode appears at negative energies, indicating the enlarged capability of the thermally excited liquid to transfer momentum and energy to the probe.[12]

IV. CONCLUSIONS

We have performed a RPA calculation of the dynamical response of liquid ^{3}He at finite temperatures. This is possible within density functional theory, provided that the multipolar components of the ph effective interaction vanish for $l\geqslant 2$; furthermore, the monopolar amplitude of this interaction has been allowed to possess a Lennard-Jones shape to make room to some finite-range effects. We have adopted a parametrization of the density functional that permits an accurate simultaneous description of the equation of state at zero temperature, the density dependence of the Landau parameters, the surface tension, and the anomalous dispersion of zero sound at vanishing temperature and at various pressures, and that guarantees stability of small drops.

The calculations here presented illustrate the applicability of the finite-temperature RPA formalism[12] to liquid helium. On the one hand, our results show that the zero-sound peak is rather sensitive to thermal broadening (cf. Fig. 6); however, experimental widths are mostly due to coupling of the collective mode to multipairs whose sizes, which range between 0.1 and 0.5 meV,[13] completely absorb the effects of thermal smoothing of the Fermi sea. It is also important to keep in mind that these experimental widths appear at any transferred momentum. On the other hand, the calculated zero-sound and paramagnon centroids agree reasonably with data. The latter exhibits a weak temperature dependence; thermal flattening of the maximum magnetic strength is more significant and also consistent with experimental results.

An important feature of measured total intensities is the large strength lying, at all temperatures, between the density and spin peaks, a fact that has been regarded as a fingerprint of a reduced value of the helium effective mass to about $2m$.[13] The present results include the effective mass that corresponds to the density at SVP for each temperature, which remains always close to $2.8m$, and do not reproduce the intermediate strengths at $T=0$ and 1.2 K. Neither can these calculations describe the measured strength at high ω, which has been attributed to multipair excitations.[19] It should be kept in mind that our formalism does not include any effect of collisional broadening of the collective mode. Although

the latter could be accounted for, at the cost of some extra numerical effort, simply considering complex energies ω in the finite-temperature RPA formalism, such a treatment would require the introduction of the imaginary part of the energy as a parameter that mimics the collisional width. A more adequate theory of collisional broadening can be developed within the RPA philosophy and will be postponed for future work, aiming at a description of the well-established variation of the zero-sound width with increasing pressure.[17]

Finally, we wish to stress that our calculated strength exhibits a negative energy tail extending up to -0.5 meV, in good agreement with existing data.[18]

ACKNOWLEDGMENTS

This work was partially supported by CONICET and UBA (Argentina) through Grant Nos. PID 34520092 and EX100, and by DGICYT (Spain) through Grant Nos. PB92-0761 and PB92-0820.

[1] S. Stringari, Phys. Lett. **106A**, 267 (1984).
[2] S. Stringari and J. Treiner, Phys. Rev. B **36**, 8369 (1987).
[3] S. Stringari and J. Treiner, J. Chem. Phys. **87**, 5021 (1987).
[4] Ll. Serra, J. Navarro, M. Barranco, and Nguyen Van Giai, Phys. Rev. Lett. **67**, 2311 (1991).
[5] C. García-Recio, J. Navarro, Nguyen Van Giai, and L.L. Salcedo, Ann. Phys. (N.Y.) **214**, 293 (1992).
[6] D. Pines, Can. J. Phys. **65**, 1357 (1987).
[7] S. Weisgerber, P.G. Reinhard, and C. Toepfer, in *Spin Polarized Quantum Systems*, edited by S. Stringari (World Scientific, Singapore, 1988), p. 121.
[8] J. Dupont-Roc, M. Himbert, N. Pavlof, and J. Treiner, J. Low Temp. Phys. **81**, 31 (1990).
[9] S. Weisgerber and P.G. Reinhard, Phys. Lett. A **158**, 407 (1991).
[10] E.S. Hernández, M. Barranco, and A. Polls, Phys. Lett. A **171**, 119 (1992).
[11] M. Barranco, D.M. Jezek, E.S. Hernández, J. Navarro, and Ll. Serra, Z. Phys. D **28**, 257 (1993).
[12] E.S. Hernández, J. Navarro, A. Polls, and J. Ventura, Nucl. Phys. **A597**, 1 (1996).
[13] H.R. Glyde, *Excitations in Liquid and Solid Helium*, Clarendon Press, Oxford, 1994.
[14] H.R. Glyde and F.C. Khanna, Phys. Rev. Lett. **37**, 1692 (1976); Can. J. Phys. **59**, 343 (1980).
[15] S. Greywall, Phys. Rev. B **27**, 2747 (1983).
[16] G. Baym and C. Pethick, *Landau Fermi Liquid Theory* (Wiley, New York, 1991).
[17] R. Scherm, K. Guckelsberger, B. Fåk, K. Sköld, A.J. Dianoux, H. Godfrin, and W.G. Stirling, Phys. Rev. Lett. **59**, 217 (1987).
[18] K. Sköld, C.A. Pelizzari, K. Kleb, and C.E. Ostrowski, Phys. Rev. Lett. **37**, 842 (1976); K. Sköld, and C.A. Pelizzari, Philos. Trans. R. Soc. London B **290**, 605 (1980).
[19] F. Dalfovo and S. Stringari, Phys. Rev. Lett. **63**, 532 (1989).
[20] D. Pines and P. Nozières, *The Theory of Quantum Liquids I: Normal Fermi Liquids* (Benjamin, New York, 1966).